Titre: Title:	Manufacturing of the aluminum metal-matrix composite reinforced with micro- and nanoparticles of TiO₂ through accumulative roll bonding process (ARB)
Auteurs: Authors:	Razieh Yousefian, Esmaeil Emadoddin, & Sadreddin Baharnezhad
Date:	2018
Type:	Article de revue / Article
Référence: Citation:	Yousefian, R., Emadoddin, E., & Baharnezhad, S. (2018). Manufacturing of the aluminum metal-matrix composite reinforced with micro- and nanoparticles of TiO₂ through accumulative roll bonding process (ARB). Reviews on advanced materials science, 55 (1), 11 pages. https://doi.org/10.1515/rams-2018-0022

Document en libre accès dans PolyPublie
Open Access document in PolyPublie

URL de PolyPublie: PolyPublie URL:	https://publications.polymtl.ca/5185/
Version:	Version officielle de l'éditeur / Published version Révisé par les pairs / Refereed
Conditions d'utilisation: Terms of Use:	CC BY-NC-ND

Document publié chez l'éditeur officiel
Document issued by the official publisher

Titre de la revue: Journal Title:	Reviews on advanced materials science (vol. 55, no. 1)
Maison d'édition: Publisher:	Walter de Gruyter
URL officiel: Official URL:	https://doi.org/10.1515/rams-2018-0022
Mention légale: Legal notice:	

MANUFACTURING OF THE ALUMINUM METAL-MATRIX COMPOSITE REINFORCED WITH MICRO- AND NANOPARTICLES OF TiO$_2$ THROUGH ACCUMULATIVE ROLL BONDING PROCESS (ARB)

Razieh Yousefian[1], Esmaeil Emadoddin[1] and Sadreddin Baharnezhad[2]

[1]Faculty of materials and metallurgical engineering, Semnan University, Iran
[2]Department of mechanical engineering, École Polytechnique de Montréal, Canada

Abstract. The aluminum metal-matrix composites reinforced with the micro- and nanoparticles of TiO$_2$ were manufactured in the form of sheets through the accumulative roll bonding (ARB) process which has been lately considered as a novel method under an intense plastic deformation so as to produce particulate-reinforced metal-matrix composites. The microstructural examinations via optic microscopy and scanning electron microscopy (SEM) depict that the distribution of TiO$_2$ particles in the aluminum matrix is almost uniform and also the dispersion of the microparticles of TiO$_2$ is more homogeneous than that of the nanoparticles one. Furthermore, the tensile tests demonstrate the noteworthy enhancements in the tensile strengths of the composites, compared to the Al 1100 as the virgin metal, however, by attenuating the size of the particles, i.e. from micron to nano, the composite tensile strengths are augmented. The fractographic analysis of the fracture surfaces revealed that the fracture mode in the ARB-processed Al/TiO$_2$ composite is the shear ductile rupture type.

1. INTRODUCTION

Metal-matrix composites are a generation of engineering materials which have been the subject of several researches in the recent years. By virtue of their good properties, they are widely used in military and automotive industries [1-3]. General properties of aluminum alloys such as low density, appropriate corrosion, resistance and mechanical properties; have made them appropriate candidate as a matrix in more commercial metal matrix composites [4]. Reinforcements are mostly included in different types of carbides (e.g. SiC and B$_4$C), nitrides (e.g. Si$_3$N$_4$ and AlN) or mechanical properties of metal matrix composites depend upon the nature, volume fraction, particle size, morphology and distribution of reinforcements [5,6]. Several theories have been proposed to explain the relation between the volume percentage and shape of particles with distance between them [7-9].

Accumulative roll bonding (ARB) is an intense plastic deformation process applied as a novel method to produce particle reinforced metal matrix composites now. Roll bonding of the metallic sheets with a thin layer of reinforcement powder between them is the main stage in this process. The quality of the bonding achieved has a crucial role in the properties of the products. Kitazono et al. [10] developed the ARB process for fabricating the metal foams. During the ARB process, they added the TiH$_2$ powder between two metallic layers and with repeated passes of ARB. These particles were dispersed uniformly and finally the product sheet was treated under foaming heat treatment. Lee et al. [11]

Corresponding author: S. Baharnezhad, e-mail:sadreddin.baharnezhad@polymtl.ca

used the ARB process in order to improve the distribution of SiC particles in the aluminum-matrix and produced an ultra-fine grain micro-structure in Al/SiC composite. Alizadeh et al. [12] used this idea to fabricate the Al/SiC composites via the repeated roll-bonding (RRB) and the continual annealing roll-bonding (CAR) process. The RRB is distinguished by annealing of sample between each pass which eliminates the effects of prior work hardening. Anodizing followed by the ARB process for manufacturing of Al/Al$_2$O$_3$ composites was also used by Jamaati et al. [13]. Lu et al. [14] successfully applied similar method to produce the Al/SiO$_2$ composite. Rezayat et al. [15] used the ARB method to produce the high strength Al/SiC nanoparticle composite.

So far, little research has been carried out on the fabrication of composites reinforced with the sub-micro and nanoparticles through ARB process by studying the effect of particle size on the microstructure, the mechanical properties, the bonding strength, the distribution of reinforcing particle thorough the matrix and the mechanism of powder dispersion during forming process .Accordingly, in this research, the aluminum-matrix composites reinforced with the micro- and nanoparticles of TiO$_2$ were fabricated by the ARB process. The microstructure and the mechanical properties of the composites were investigated and the mechanisms of the particle dispersion during the fabrication process and the fracture mode were also studied.

2. EXPERIMENTAL PROCEDURE

Some aluminum sheets of 1100 alloy with the size of 1×50×150 mm^3 were used. To remove the effect of work hardening of the base metal sheets and improve the bonding of particles with the metal at the interfaces, the sheets were heated at 623K, in a furnace at the ambient atmosphere for 1 hour, and then, cooled in the furnace. Table 1 shows the

Table 1. Chemical composition of the examined sheets, wt. %.

Grade	Al	Si	Fe	Cu
Al 1100	99.15	0.15	0.52	0.15

chemical properties of the Al sheets. The mechanical properties and the after-annealing fracture strain of the sheets yielded from the tensile tests have been shown in Table 2. In order to investigate the effect of reinforcement particle size on the properties of composites produced by ARB route, TiO$_2$ particles were used with two different sizes: less than 30 μm and 50 nm.

For preparation of the composites, firstly, the bonding surfaces between the two sheets were completely degreased with acetone, and then, the sheet surfaces were smoothed with a stainless steel brush with a wire diameter of 0.4 mm. For the both particle sizes, 0.5 wt.% of TiO$_2$ powder was distributed almost uniformly between these surfaces of two aluminum sheets using the wire sieve. After the temporary joining of the initial sandwich by copper wire, the sample was cold rolled for the first time with the thickness reduction of 60% and a speed of 10 rpm. This operation was carried out at the room temperature by a laboratory mill of 110 mm roll diameter without using any lubricant in order to improve the distribution of the TiO$_2$ particles in the aluminum matrix, and consequently, enhance the bonding strength. In the second step, the produced samples in the first pass were divided into two equal parts along the rolling direction (RD) and the whole process for the last steps was repeated except adding the powder. This process (ARB) was repeated up to 7 cycles to produce Al/TiO$_2$ composites with a 50% reduction in thickness and a speed of 10 rpm, without preheating or inter-pass annealing (In the first cycle, in order to establish the proper connection with a suitable strength between the layers of sheet and reinforcement powder, 60% reduction was used. And in the next cycles, to distribute the reinforcement particles which had been used in the first cycle, 50% reduction was used). To detect and confirm the presence of TiO$_2$ particles in the composite, the EDAX analysis was used. A typical result is depicted in Fig. 1. Considering the particle sizes and difficulty in using EDAX spot analysis, the area selected contains the TiO$_2$ particles. According to the chemical composition of the base metal (Table 1) and the production procedure, the Ti peak in the EDAX analysis only refers to the presence of titanium oxide in the structure.
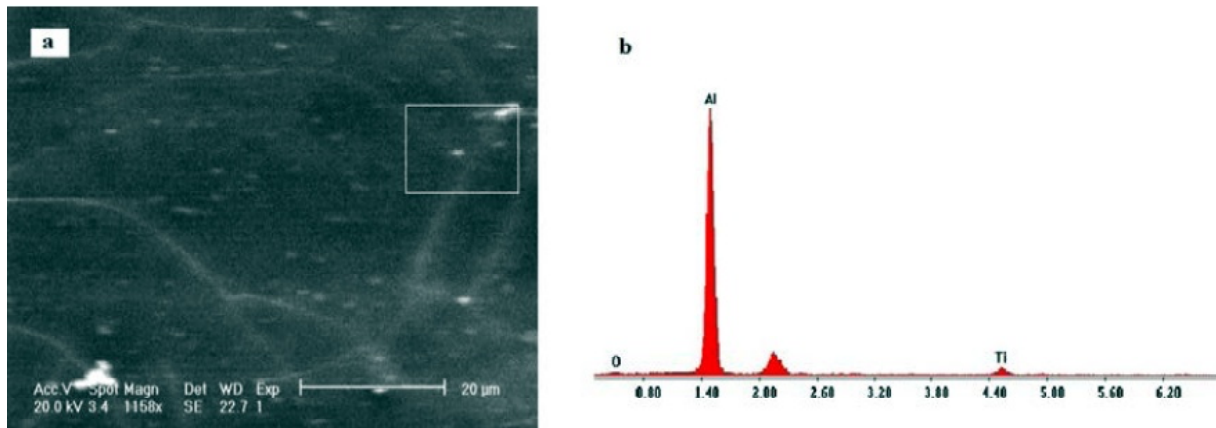
Table 2. The mechanical properties of the sheets examined.

Grade	Ultimate Tensile Strength (MPa)	Yield Strength (MPa)	Elongation (%)
Al 1100	59.5	24.9	24

Fig. 1. TiO_2 detection in the Al-0.5 wt.% TiO_2 composite (a) the SEM micrograph and (b) the EDS analysis.
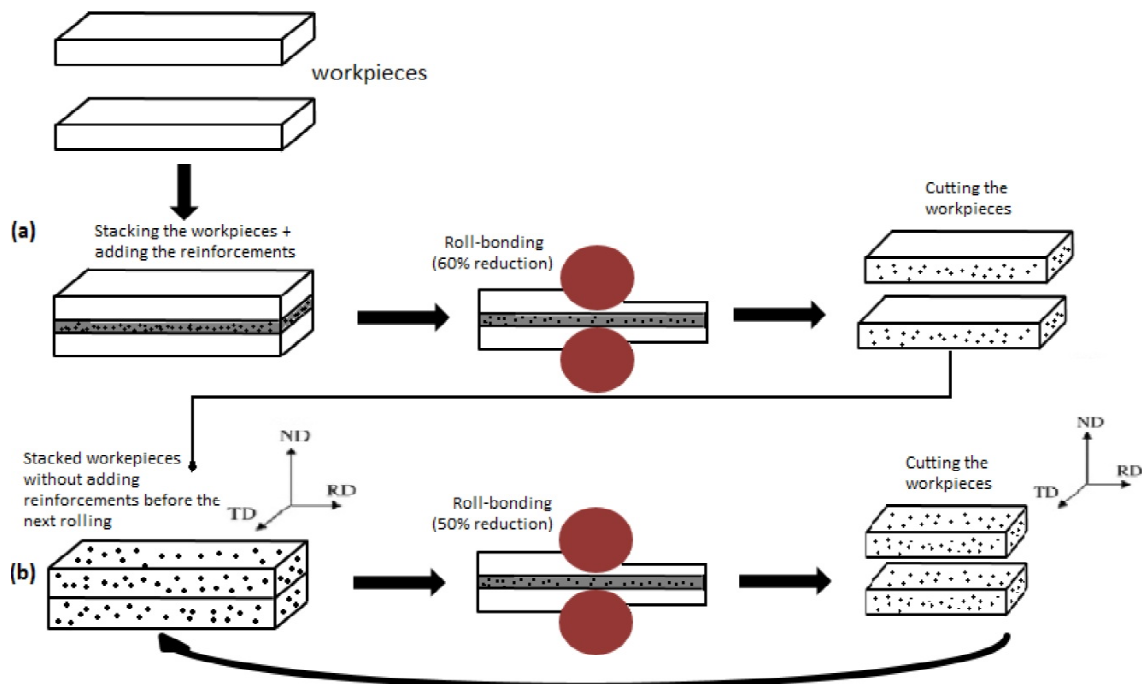

Fig. 2. Schematic illustration of the production route of the Al/TiO_2 composites sheet through the ARB process: (a) first step and (b) second step.

For microstructural observations and their changes during different cycles and also to study the fracture surfaces of tensile test specimens, optical microscopy (OLYMPUS2-UMA) and scanning electron microscopy (CamScan MV 2300) were used, respectively. After preparation of the composites, sub-size tensile test samples from various cycles of ARB parallel to the rolling plane (RD–ND (rolling direction–normal direction) plane) were cut by wire cut machine with a gauge length of 12.5 mm and a width of 4 mm as per the standard of ASTM E8 [16]. The uniaxial tensile tests were carried out using a tensile testing machine model Zwick/ZO50 with a jaw speed of 0.5 mm/min at the room temperature. After conducting the uniaxial tensile tests on the samples, fracture surfaces were

analyzed to determine the fracture mechanism. Fig. 2 depicts schematically the process in first and second step.

3. RESULTS AND DISCUSSION

3.1. Microstructural observations

The light microscope images of the RD-ND section, Fig. 3, illustrate the mechanism of interlayer bonding in the first stage of the ARB process. At the initial cycles, the powder layers broke up to the small fragments and the virgin metal was extruded through the fragments. In which it can be seen that the powder layer has been broken and the matrix metal extruded through the cracks. This phenomenon is the main mechanism of particle distributions in the
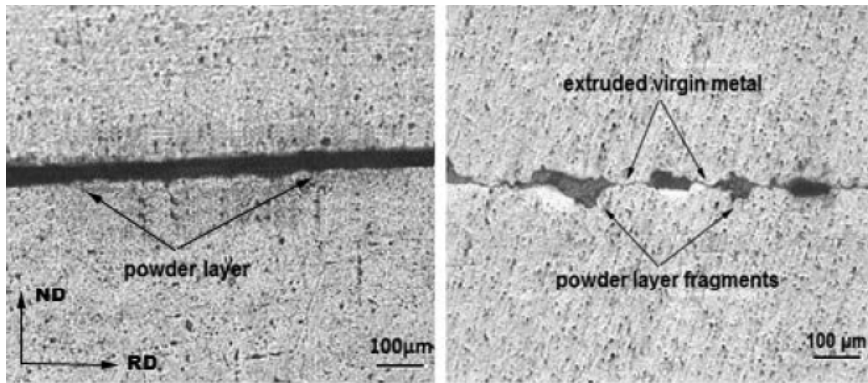
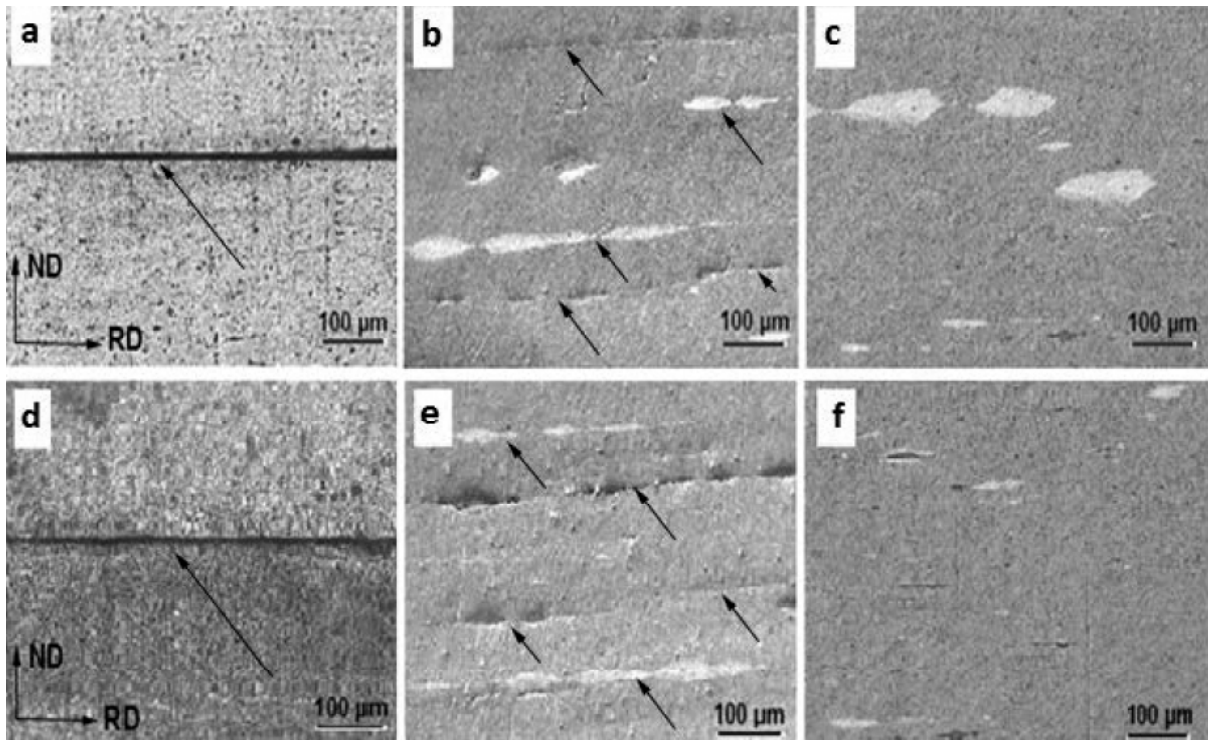**Fig. 3.** The light micrographs of (a) initial stack and (b) after the second pass of rolling.

Fig. 4. The light micrographs of Al-0.5 wt.% TiO$_2$ reinforced with (a,b,c) micron, and (d,e,f) nano particles produced by first (a,d), third (b,e) and seventh (c,f) cycles of ARB process.

successive cycles. Thus, with increasing number of cycles, powdery layer is frequently broken, and consequently, in the final cycles, all particles would be distributed in the bulk of matrix. The particles among layers hinder this mechanism. The extrusion of base metal in the crack of layer would be prevented by the presence of TiO$_2$ particles. Moreover, plastic flow of materials near to the surface would be more difficult when they have been strengthened by nanoparticles.

Fig. 4 depicts the microstructure variations of composites reinforced with micro- (a, b, c) and nanoparticles (d, e, f) of TiO$_2$, which have been produced by different cycles of the ARB process. It is observed that the deformation causes more uniform distribution of powder layers and also extrusion of

the matrix through reinforcement particles. With further deformation, the surface area of the region containing the powders would be reduced and the matrix flows through the agglomerated particles. It should be noted that the bright color regions in images demonstrate the interface between the layers.

Extending the number of the process cycles, the interface related to the primary cycles is disappeared and only the interface of layers related to the last cycles can be detected in the center of the sample.

Plastic flow in the region near to agglomerated particles is significantly less than the matrix and the plastic flow around them causes shear to them. Particles that are located at the interface of layers
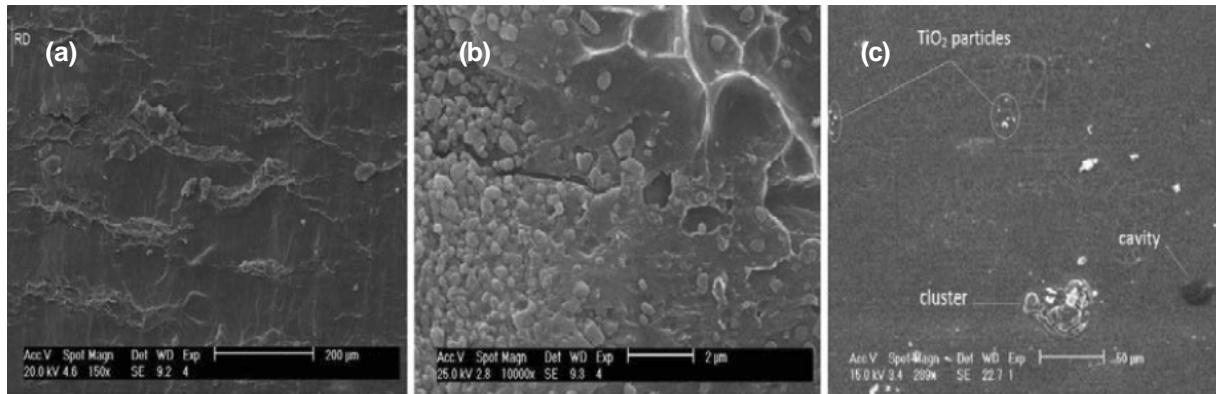
Fig. 5. The SEM micrograph of (a,b) the peeling surface and (c) side section of the Al-0.5 wt.% nanoparticles of TiO_2 after seven ARB cycles.

and are usually agglomerated have fewer restrictions than the particles that are dispersed within the matrix. Therefore, by the shear stress that the matrix applies, the stream begins move in the RD-ND direction and disperse between layers. As a result, by increasing the deformation of each cycle, these regions gradually disappear and a structure with a uniform distribution of the particles will be generated [17].

At the initial cycles of the ARB process, bonding interface is engaged by TiO_2 particles which decrease the bond strength and the mechanical properties. Raising the number of ARB cycles, along with more dispersion of the particles, improve the initial bonding of interfaces, and therefore, a relatively integrated structure will be created in the final cycles. As it is depicted in Fig. 3, fragments of the powder layer are totally disappeared in the last cycles of ARB process. It can be seen that after 7 cycles, there is no trace of the original layered structure. In addition, to the dispersion of the initial particles layer, growing up the number of metal layers is another factor in the improvement of the particle distribution [14].

Evidences of extrusion in the base metal through the powder layer fragments are observed in the SEM micrographs (Figs. 5a and 5b). Generally, all defects that are observed in the structure can be categorized into four groups: reinforcement particle agglomeration, non-uniform distribution zones, the cavities that are formed at the interface and the retained fragment of primary particles between sandwich layers (Fig. 5c). It was determined that the mechanical properties of the composites are seriously affected by the presence of different types of defects in the microstructure [2,18]. At early cycles of the ARB process, the presence of TiO_2 particles at the interface of the aluminum layers causes de-

creasing of the bond strength. Furthermore, the dispersion of powder in the matrix is obtained through more deformation, and thus, the presence of agglomerates is foreseeable. Moreover, the matrix is severely strain hardened. Hence, a severe reduction of the fracture strain at primary cycles seems reasonable. Agglomeration of the particles in the structure leads to decrease the real reinforcement in matrix and so the inter-particle distance gains. In addition, these places are capable of producing nucleation and growth of the cracks during the tensile test. Presence of the clusters raises the local stresses and the number of voids and facilitates their linkage [18,19]. In fact, these defects are contributed to decrease the strength and fracture strain. However, it is clear that by reducing the size of reinforcement particles, the bond strength at the interface of the layers is reduced. As it was stated formerly, more deformation of the composite causes to remove the porosity, removal of the powder layer fragments, and particle agglomeration and clusters. This, in turn, leads to enhance the bond strength between the aluminum layers. Thus, raising the ARB cycles is led to lower defects number in the microstructur, which causes to improve the elongation of the produced composite.

Fig. 6 depicts that the particle size diminishes, the retained fragment of the initial powder layer is increased. The cause of this defect goes back to initial stack bonding during the first cycle of rolling. At this stage, for the fine particle size and/or thick initial powder layer, the each other. This phenomenon leads to create the fragment of particles layer with identical dimensions. Proceeding the deformation, these elongated fragments are gradually configured into an ellipsoidal shape, and the matrix material will flow easily over them. These ellipsoidal fragments would be stable and without any more
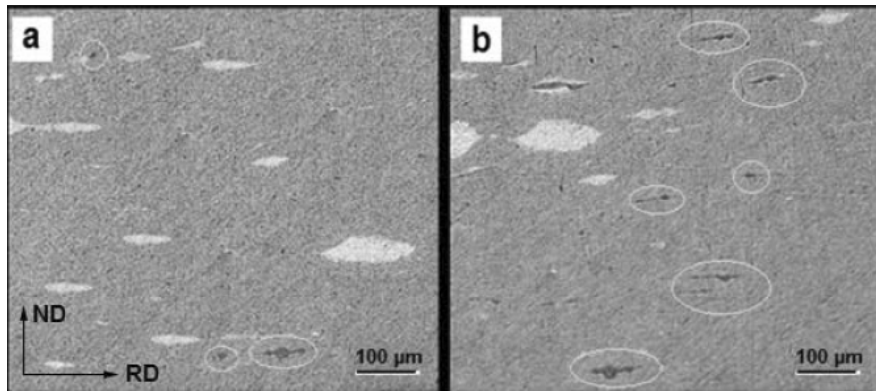
Fig. 6. The light micrographs of retained fragment of the initial powder layer after seven cycles of the ARB (a) microparticles and (b) nanoparticles.
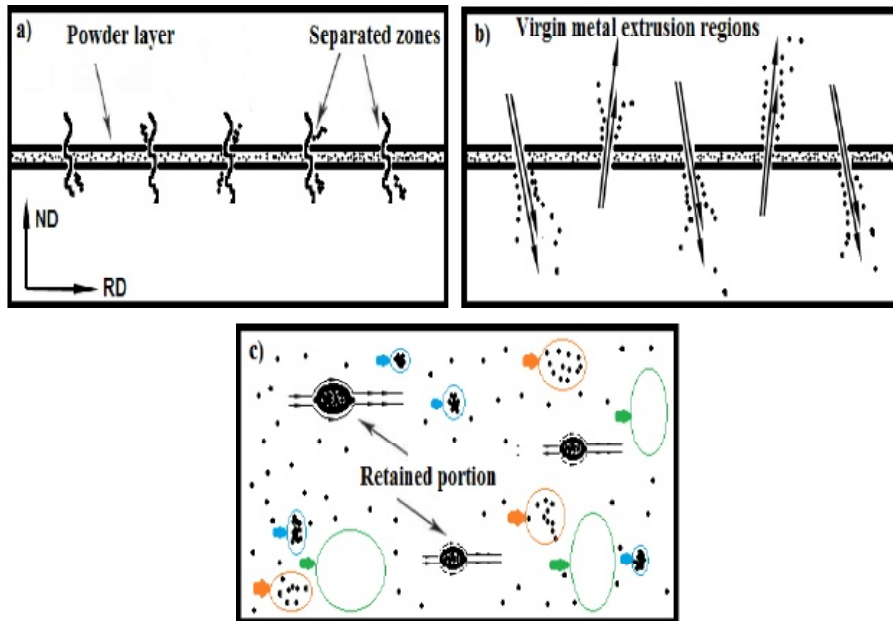

Fig. 7. The schematics of powder layer separation and dispersion of particles in (a) matrix (b) initial cycles and(c)final cycles of ARB.

dispersion even at higher cycles of ARB. Indeed, matrix prefers to flow over the particle cluster rather than the flowing between them, Fig. 7.

On either side of the defect, because of the applied compressive stress [20], and also the presence of effects of primitive interface, in addition to the reasons aforementioned, cracks are created so that results decrease strength and fracture strain. To eliminate these defects, it shall reduce the initial amount of particles between the aluminum sheets, and also increase the number of process cycles.

3.2. Mechanical properties

In order to evaluate the mechanical properties of composites reinforced with micro-and nanoparticles produced by the ARB process, the tension test samples were prepared in the certain passes and in the

rolling direction (RD). The results of the tensile test are presented in Fig. 8. According to these diagrams, the elongation of the initially annealed Al/TiO$_2$ laminate has been dramatically reduced and increased slightly after the every cycle. Reducing the ductility at primary cycles can be due to a highly strain hardening, non-uniform distribution of particles, presence of agglomerates of particles in the matrix, and finally because of inadequate bonding at the interface. The enhancement of the ductility by the ARB cycles is essentially by courtesy of altering the layered structure and particle agglomeration and dispersion of theTiO$_2$ particles in the matrix, and also improving the bond strength between the layers. As shown in these graphs, in both composites, the strength builds up by increasing the number of ARB cycles. Likewise, the total elongation of composite is augmented by extending the number of cycles
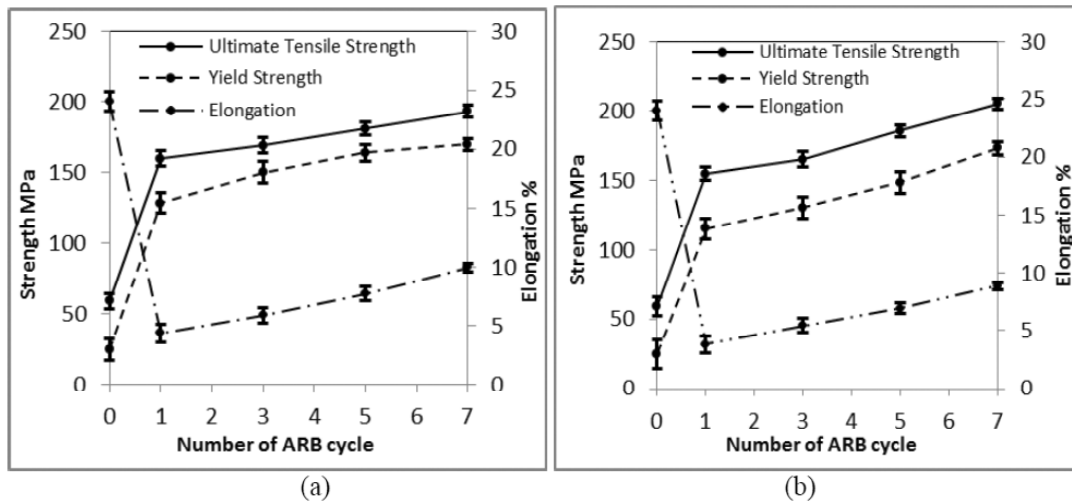
Fig. 8. The mechanical properties results of the Al-0.5wt.% TiO_2 composites with (a) microparticles and (b) nanoparticles.

justifying this behavior we can mention such items: improvement of bonding strength between layers of aluminum and titanium dioxide, reducing the interfacial cavities, reducing the clustering of particles, a more uniform distribution of the reinforcing particles which result in the more uniform deformation of specimen. Therefore, the number of ARB cycles is raised, the defects in the microstructure are decreased and the bonding quality is improved, which cause to boost the mechanical properties of the produced composite [15,21]. These factors will grow elongation by extending the number of the process cycles.

In the early cycles (less than 3 cycles) of the ARB process, dislocation strengthening, as a result of forming the sub grains with small misorientations, plays an important role to augment the strength of the material. Extending the number of ARB cycles, the role of dislocation strengthening is gradually lowered and strength enhancement is mainly attributed to the formation of ultra-fine grain structure with high misorientations as the grain refinement mechanism [22,23]. The reports showed that after six cycles of ARB, the strengthe was saturated by reason of emersion of a ulta-fine-grained microstructure.

According to Fig. 8, it is observed that after the sixth cycle, the yield and ultimate strengths are slightl improved. This means that saturation of the strength as the result of ultrafine grains in all microstructure may occur before the sixth cycle. Therefore, building up the strength proceeds until the defects of the matrix are removed via deformation. These findings are consistent with those reported by the researchers referenced above. As it was mentioned, using finer particles makes it difficult to

dispense them in structure, and more ARB cycles are needed for saturation of strengthening. In other words, in composite which contains larger particles, the strengthening saturation occurs in less ARB cycles [21].

It was suggested that when the composite is plastically deformed, a geometrical mismatch will be produced in light of deformation-induced plastic strain gradient around the particles in matrix. This mismatch is relaxed by formation of dislocations which are geometrically necessary. As what aforementioned, the density of geometrically necessary dislocations in the deformed material is a function of the average tensile strain of the matrix and average distance among the particles [7,24]. Actually, in view of the variations of temperature during the production process, geometrical dislocations will be generated to accommodate the strain incompatibility around the particles [25]. Hence, owing to low rolling temperature and small differences between the thermal expansion coefficients of the particles and the matrix, influence of variation in temperature of dislocation density is dispensable. The presence of more dislocations in the structure and interaction between them leads to expand the work hardening of the composite. Development of the ultrafine grains in the composite is easier than the unreinforced matrix alloy [11] as well. Meanwhile, the small TiO_2 particles act as the barriers to dislocation movements during deformation and by passing dislocations via the particles, ''Orowan'' loops will be left behind causing the higher yield strength [26].

Changes of tensile strength and elongation in the composites reinforced with micro- and nanoparticles are compared in Fig. 8. In order to evaluate the contribution of each above mentioned
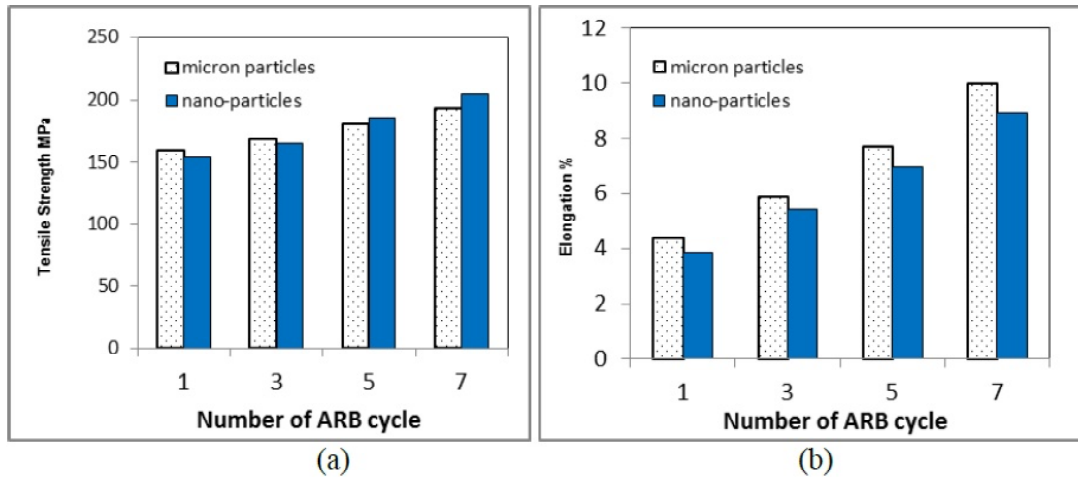
Fig. 9. The comparison of (a) the tensile strength and (b) the elongation of the composites with the different reinforced particle sizes.

mechanisms, a comparison has been made between the tensile strength of the two kinds of composites produced in this research and the ARBed Al 1100 by Rezayat et al. [15]. The tensile strength values of the aluminium-matrix composites reinforced with the micro- and nanoparticles after seven and eight ARBed cycles have been measured 193.5 MPa (μm), 204.7 MPa (nm), and 186 MPa, respectively [15]. Thanks to the similar specifications of Al 1100 strips used in this research with the one used by Rezayat's work (59.5 MPa and 57.6 MPa, respectively), their results were chosen for comparison, in spite of this fact that they have not reported the tensile strength of the ARBed aluminum after seventh cycle. It is clear that composites reinforced with micro- and nanoparticles after seven ARB cycles exhibit a higher tensile strength than ARBed aluminum after eight cycles. Indeed, TiO_2 particles can effectively enhance the strength of the matrix, even with a very low weight percent (0.5%), when it has been uniformly dispersed in the aluminum matrix as can be achieved by the ARB method.

As shown in Fig. 9, in both composites, by extending the number of process cycles, the tensile strength boosts. Besides, in both diagrams, from the third to fifth cycles, a sharp growth in the tensile strength was recorded, which is probably because of extending in the number of cycles. The reinforcement particle distribution and initial bonding of interface are improved and the laminated structure (the Al sheets and powder layer) is replaced with a relatively integrated structure. Here the significant point is that, up to the third cycle, the mechanical properties, especially, the tensile strength of composites reinforced with nanoparticles are less than the mechanical properties of microparticle-reinforced

composites; but from third to fifth cycles, more variations are observed in the mechanical properties of composite reinforced with nanoparticles in comparison with other composite. As noted above, agglomerates and non-uniform particle distribution areas in the sample reinforced with nanoparticles are more probable, and the only way to eliminate these defects is increasing the amount of accumulated strain and applying the higher number of cycles of the process.

By increasing the number of cycles, clustering and agglomeration of nano-powder particles are decreased partially and by reducing these defects, a significant improvement is observed on the mechanical properties.

Comparing the tensile properties of the two composites shown in Fig. 9, it is also implied that the strength of composites by using two different particle sizes is similar and close together. Based on the findings of other investigations, using the nano-size particles, however, leads to further improvement in the strength of the composite, it will also expand the possibility of creation of microstructural defects [20,27,28].

Expanding the number of cycles, the elongations are gained for both types of composites. In the composite reinforced with microparticles, the maximum increase is observed in third to fifth cycles, which may be by reason of the optimum uniform distribution of microparticles which took place among these cycles. The first two cycles and the last two cycles had a smaller contribution in uniform distribution of the reinforcing powder particles. But, in the structure of the composite reinforced with nanoparticles, a gradual trend and improvement is observed by extending the number of cycles. In fact, each cycle
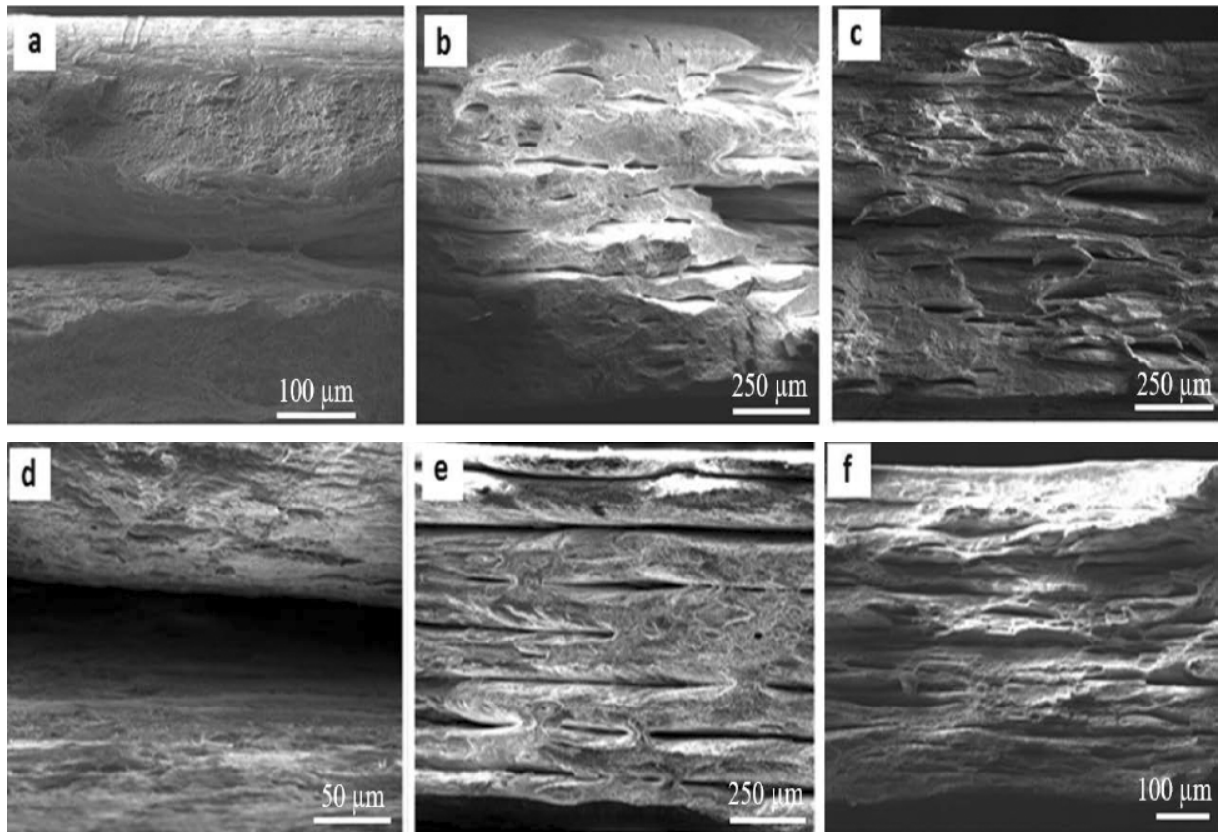
Fig. 10. The SEM images (150x and 300x) lead up to the fracture surface of the composites reinforced with micro- (a, b, c) and nanoparticles (d, e, f) produced after (a, d) first, (b, e) five and (c, f) seven cycles of the ARB process.

of the ARB has an effect on the distribution of powder reinforcement particles and the number of clusters will decrease while it still has the ability to get more uniform.

3.3. Fractography

Scanning electron microscopy (SEM) was used for investigation of the fracture surfaces of the samples in the different cycles of accumulative roll bonding. The fracture surfaces of after-uniaxial tensile tests were studied in order to determine the fracture mechanism. In Fig. 10, the SEM images, in the low magnifications, are pertinent to the fracture surfaces of the composites reinforced with the micro- and nanoparticles using the ARB process in the three different cycles.

As it can be seen, the bonding strength is very low in the initial cycles of the process, so that the separation between the layers occurs in a wide area. In sample processed at the first cycle, separation between the layers of the samples can be observed well in some areas. Owing to the higher area of dispersion of nano-sized particles than micro-sized particles, in the sample reinforced with

nanoparticles, even in the higher cycles of the ARB, the separation between the sample layers is quite distinctive in some areas. It is determined that whatever the numbers of cycles extend, the interlayer separation decreases, and consequently, the bonding strength significantly enhances.

The higher magnification of the fracture surfaces in the different cycles of the ARB are provided in Figs. 11a-11c. It can be seen that by increasing the number of cycles, the fracture mode, which is almost the soft at the primary cycles, will be changed to the brittle mode at the last cycles. As it was seen, the bonding quality controls the mechanical properties as well as the fracture mechanism of the composites [18,19]. Indeed, mechanical interlocks are formed between the adjacent surfaces at the interface of the particle matrix. It was mentioned that the flow of the matrix around the particles in the high pressure and temperature can improve the bond strength of the matrix and particles [21]. In this way, by seven ARB cycles, the strong mechanical bonding between the matrix and particles is expected, and it can be approved by the presence of most of the particles after polishing of the surface (Fig. 5c) and also on the fracture surface
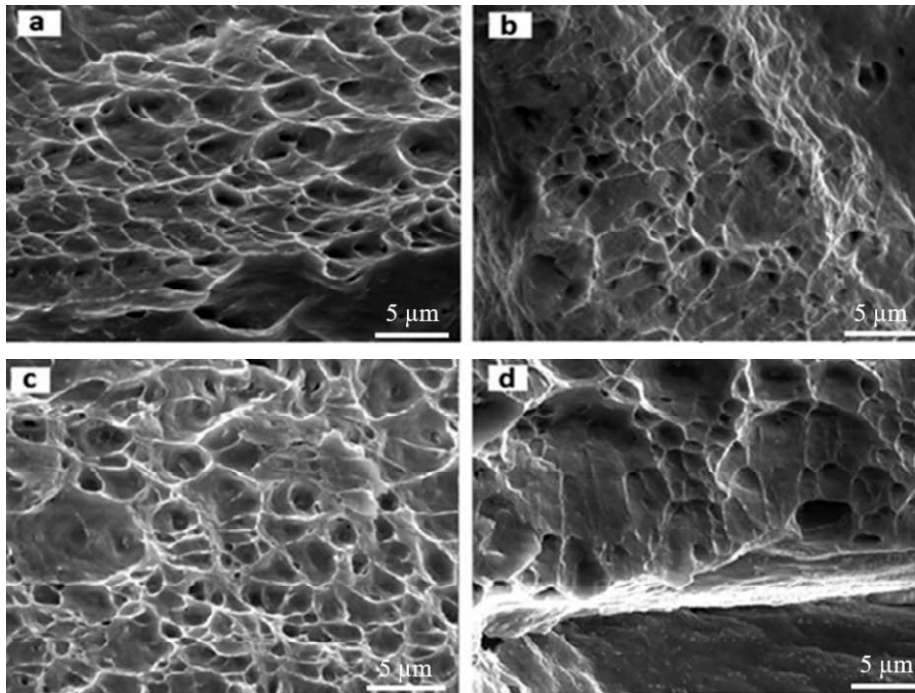
Fig. 11. The SEM images (5000x) of the fracture surfaces of the composites reinforced with micro- (a, b) and nanoparticles (c, d) fabricated by (a, c) first and (b, d) seven cycles of the ARB process.

after the tensile test (Fig. 11). Of course, in these composites, due to the use of the fine spherical reinforcements with a high strength, the fracture of the particle is not likely to occur [18,19]. Moreover, owing to the high strength of the work-hardened base metal, decohesion of the matrix-particle interface is more likely than the fracture of the matrix during the tensile test. Therefore, nucleation of voids at the matrix-particle interface and their growth is the fracture mechanism. Fracture will occur by coalescing the voids and the shear between them in a matrix [15]. Deep and elongated dimples are the result of the nucleation of micro- voids, their consequent growth in the structure, and finally their coalescence, which is affected by shear stress [29]. Also, TiO_2 particles have a significant effect on the fracture surface of the composite. The presence of TiO_2 particles in the walls and core of most dimples means that the matrix- particle interface and particle agglomeration provided suitable sites for crack initiation and propagation. Crack propagation took place by decohesion at the matrix-particle interface as a weak place in the structure [18,19].

The comparison between the fracture surfaces of two composites with micro- and nano-sized particles indicates that particle size is decreased, cavities number is grown while their dimensions decrease. This phenomenon is caused by decreasing the distance between particles and increasing ma-

trix-particle interface as a suitable place for nucleation of cracks or cavities.

In high cycles, building up the strength, work hardening of metallic layers and decreasing the elongation of them, leads to reduce the number of micro-cavities (dimples) at the surface. Therefore, the same limited numbers of remaining dimples have a low depth with shear orientation, and the fracture mode becomes similar to brittle fracture, which is associated with the creation of flat fracture. In general, it can be noted that the fracture mode is a shear ductile rupture (gray fibrous with dimples).

4. CONCLUSIONS

The aluminum composites reinforced with the 0.5 wt.% TiO_2 particles were successfully fabricated with the micro- and nano-sized particles after seven cycles of the ARB. The microstructure and the mechanical properties of the composites were investigated and the results of this study are summarized as follows:

− By increasing the cycles number of the ARB process, the distribution of the reinforcing particles in the matrix were more uniform and the defects which usually exist in the composites structure were reduced.

− Moreover, by extending the cycles, the composite sheet will be progressively formed, and in the

seventh cycle, the tensile strength of composites reinforced with the micro- and nano-sized particles, reached to 193.5 and 204.7 MPa, respectively, whereas the after-annealing tensile strength of the primary aluminum was 59.5 MPa.

− By atenuating the size of reinforcing particles and reducing the distance between them, the structural defects will be raised.

− The SEM observations of the fracture surfaces revealed that the fracture mode in the ARB-proc-essed Al/TiO$_2$ composite is shear ductile rupture type.

− After one pass of the ARB process, the ductility (elongation) of the samples drastically diminished from 24% to 4.38% (μm) and 3.85% (nm), and after seven cycles, then, approached to 9.99% (μm) and 8.91% (nm).

ACKNOWLEDGEMENT

REFERENCES

[1] S.V. Prasad and R. Asthana // *Tribol. Lett.* **17** (2004) 445.

[2] T.S. Srivatsan, I.A. Ibrahim, F.A. Mohamed and E.J. Lavernia // *J. Mater. Sci.* **26** (1991) 5965.

[3] E. S. C. Chin // *Mater. Sci. Eng. A* **259** (1999) 155.

[4] S.V. Kamat, J.P. Hirth and R. Mehrabian // *Acta Metall.* **37** (1989) 2395.

[5] L.M. Tham, M. Gupta and L. Cheng // *Mater. Sci. Eng. A* **354** (2003) 369.

[6] T.J.A. Doel, M.H. Loretto and P. Bowen // *Composites* **24** (1993) 270.

[7] M Kouzeli and A. Mortensen // *Acta Mater.* **50** (2002) 39.

[8] M. Rahimian, N. Ehsani, N. Parvin and H.R. Baharvandi // *Mater. Des.* **30** (2009) 3333.

[9] F. Tang, M. Hagiwara and J.M. Schoenung // *Mater. Sci. Eng. A* **407** (2005) 306.

[10] K. Kitazono, E. Sato and K. Kuribayashi // *Scr. Mater.* **50** (2004) 495.

[11] S.H. Lee, C. Lee and S.Y. Chang // *Mater. Sci. Forum* **449-45** (2004) 613.

[12] M. Alizadeh, M. Paydar, M. Alizadeh and M.H. Paydar // *J. Alloys Compd.* **477** (2009) 811.

[13] R. Jamaati, M.R. Toroghinejad and A. Najafizadeh // *Mater. Sci. Eng. A* and (2010) 3857.

[14] C. Lu, K. Tieu and D. Wexler // *J. Mater. Process. Technol.* **209** (2009) 4830.

[15] M. Rezayat, A. Akbarzadeh and A. Owhadi // *Metall. Matter. Trans. A* **43** (2012) 2085.

[16] ASTM Standard E8M-09, *Standard test methods for tension testing of metallic materials* (West Conshohocken (PA): ASTM Int., USA, 2010).

[17] N. Kamikawa, N. Tsuji, X. Huang and N. Hansen // *Acta Mater.* **54** (2006) 3055.

[18] L. Ceschini, G. Minak and A. Morri // *Compos. Sci. Technol.* **66** (2006) 333.

[19] L. Tham, M. Gupta and L. Cheng // *Acta Mater.* **49** (2001) 3243.

[20] M.T. Khorshid, S.J. Jahromi and M. Moshksar // *Mater. Des.* **31** (2010) 3880.

[21] R. Jamaati, M.R. Toroghinejad and H. Edris // *Mater. Des.* **54** (2014) 168.

[22] Y. Saito, N. Tsuji, H. Utsunomiya, T. Sakai and R. Hong // *Scr. Mater.* **39** (1998) 1221.

[23] N. Kamikawa, X. Huang, N. Tsuji and N. Hansen // *Acta Materialia.* **57** (2009) 4198.

[24] J. Shao, B. Xiao, Q. Wang, Z. Ma and K. Yang // *Compos. Sci. Technol.* **71** (2011) 39.

[25] R.J. Arsenault and N. Shi // *Mater. Sci. Eng. A* **81** (1986) 175.

[26] Z. Zhang and D. Chen // *Mater. Sci. Eng.* **483-484** (2008) 148.

[27] Y. Yang, J. Lan and X. Li // *Mater. Sci. Eng. A* **380** (2004) 378.

[28] S. Mula, P. Padhi, S. Panigrahi, S. Pabi and S. Ghosh // *Mater. Res. Bull.* **44** (2009) 1154.

[29] M. Eizadjou, H.D. Manesh and K. Janghorban // *J. Alloys Compd.* **474** (2009) 406.